TFDTLM—A New Computationally Efficient Frequency-Domain Transmission-Line-Matrix Method

Iman Salama and Sedki M. Riad, *Fellow, IEEE*

***Abstract*—In this paper, a new computationally efficient frequency-domain transmission-line matrix (FDTLM) approach is introduced. The new approach combines the superior features of both the time- and the frequency-domain transmission-line matrix (TLM). It is based on a steady-state analysis in the frequency domain using transient analysis techniques and, hence, is referred to as the transient frequency-domain transmission-line matrix (TFDTLM). On the contrary, of all other frequency-domain techniques, the TFDTLM has the advantage of being able to extract all the frequency-domain information in the frequency range of interest from only one simulation. This special feature of the TFDTLM makes it computationally more efficient as compared to any other FDTLM method. The TFDTLM employs digital filter approximations for modeling wave propagation in inhomogeneous frequency dispersive media. The filters can be thought of as some type of compensation equivalent to the stubs in a time-domain transmission-line matrix (TD TLM), yet more accurate and more capable of modeling a wide variety of frequency-dependent material parameters. In addition, the TFDTLM has proven to have superior dispersion behavior in modeling lossy inhomogeneous media as compared to the TD TLM.**

***Index Terms*—Computational efficiency, frequency-domain techniques, TLM.**

I. Introduction

THE transmission-line matrix (TLM) method was initially formulated and developed in the time domain. One key issue in a time-domain analysis approach is the computational efficiency where a single impulsive excitation could yield information over a wide frequency range. Also, it may be more natural and realistic to model nonlinear and frequency dispersive properties in the time domain rather than in the frequency domain. However, in some circumstances, frequency-domain analysis may be more appealing. This might be due to the fact that traditional electromagnetics emphasizes frequency-domain concepts as frequency-dispersive constitutive parameters, complex frequency-dependent impedances, and reflection coefficients. It might be even easier and more direct to be able to model these parameters in the frequency domain rather than trying to synthesize an equivalent time-domain model. For these reasons, some work has been devoted to the development of a frequency-domain transmission-line matrix (FDTLM). One of these methods was developed by Vahldieck in 1992 [2] for the selective S-parameter computation of three-dimensional (3-D) waveguide discontinuities. Another FDTLM method was introduced by Johns and Christopoulos in 1992 [3], [4]. In both approaches, the simulation has to be repeated at every frequency point as in the case of most frequency-domain methods, to compute the response over the frequency band of interest. The two FDTLM approaches mentioned above are different in their natures and abilities. The first one [2] was, in fact, a time-domain transmission-line matrix (TD TLM) dealing with a steady-state analysis in the time domain. The method was claimed to reduce the computational time if the response is only required at distinct frequency points. The second approach [3], [4] was a true FDTLM with a steady-state analysis in the frequency domain. In this paper, a novel FDTLM approach is introduced based on a steady-state analysis in the frequency domain using transient analysis techniques and, hence, will be referred to as the transient frequency-domain transmission-line matrix (TFDTLM). In this approach, the link line parameters are derived in the frequency domain, as in [4], to satisfy all the medium parameters, including frequency-dependent parameters as well as electric and magnetic losses. The scattering matrix is derived in a way similar to any 3-D TLM node [5]. The connection between two adjacent cells, expressed in the form of delay in the time domain, is accounted for through multiplication by a propagation factor $e^{-\gamma\Delta\ell}$, where γ is the propagation constant in the medium and $\Delta\ell$ is the equivalent cell dimension. The steady-state solution is obtained through a process described in Section II. To make the TFDTLM approach computationally efficient as compared to the other FDTLM approach in [4], it was critical to maintain some relationship between the mesh response at one frequency point and any other frequency point. The goal was to be able to extract all the frequency-domain information in a wide frequency range by performing only one simulation. To achieve this, the connection between two adjacent cells expressed by $e^{-\gamma\Delta\ell}$ in each and every medium in the problem under consideration has to be expressed in terms of the propagation factor of some reference medium chosen to be the medium with the least propagation delay. This was done with the aid of

Manuscript received August 20, 1998.

The authors are with the Time Domain and Radio-Frequency Measurement Laboratory, Bradley Department of Electrical and Computer Engineering, Virginia Polytechnic Institute and State University, Blacksburg, VA 24061-0111 USA (e-mail: passant@spider01.cc.vt.edu; sriad@vt.edu).

Publisher Item Identifier S 0018-9480(00)05472-7.

digital filter approximations that can be implemented iteratively in the TLM mesh. The filters can be thought of as some type of compensation equivalent to the stubs in a TD TLM, yet more accurate and more general in modeling frequency-dependent material parameters. In Section II, the TFDTLM will be derived. Section III will discuss the technique used to overcome the problem of inhomogeneous media, multiple propagation factors, and frequency-dependent reflection coefficients. In Section IV, the dispersion behavior of the TFDTLM will be analyzed and compared to the hybrid symmetrical condensed node (HSCN) and the symmetrical super condensed node (SSCN). In Section V, the TFDTLM will be implemented in a 3-D mesh and a lossy rectangular cavity will be simulated. Section VI will discuss the intensity of computations and memory storage requirements in the TFDTLM as compared to TD TLM schemes. Section VII will include a summary and conclusions.

II. Derivation of the TFDTLM

The TFDTLM was originally inspired by the concept of bounce diagram in the time domain and the equivalent frequency-domain bounce diagram. The time-domain bounce diagram is a representation of the back-and-forth travel of a pulse through a structure with discontinuities causing reflections. The bounce diagram representation can be demonstrated by the following example. Consider a section of transmission line with characteristic impedance Z and length ℓ having discontinuities at both ends, as shown in Fig. 1. An impulse incident at time $t = 0$ and $x = 0$ propagates to the end of the line in time T. When it reaches the end discontinuity, it reflects back and propagates toward the excitation point, hits the discontinuity and reflects again, and so on. The steady-state positive-going waveform at the source position can be expressed as

$$v_o^i(t) = \delta(t) + \rho_1\rho_2\delta(t-2T) + (\rho_1\rho_2)^2\delta(t-4T) + (\rho_1\rho_2)^3\delta(t-6T) + \cdots \quad (1)$$

where ρ_1 and ρ_2 are the reflection coefficients at the two end discontinuities shown in Fig. 1. It is important to note that in (1), the reflection coefficients are assumed to be frequency independent. Otherwise, all the multiplication operations in (1) should be converted to convolution operations. The bounce diagram can also be formulated in the frequency domain by expressing every delay by the appropriate propagation factor $e^{-j\beta\ell}$ where ℓ is the length of the line and β is the wavenumber or propagation constant. The frequency response of the positive-going waveform can then be expressed as

$$V_0^i(j\omega) = 1 + \rho_1\rho_2(j\omega)e^{-2j\beta\ell} + \left(\rho_1\rho_2(j\omega)\right)^2 e^{-j4\beta\ell} + \cdots = \sum_{k=0}^{k=\infty}\left(\rho_1\rho_2(j\omega)\right)^k e^{-j2k\beta\ell}. \quad (2)$$

The frequency-domain expression in (2) holds whether or not the reflection coefficients are frequency dependent. In this problem, it appears from the above expression that if the reflection coefficients ρ_1 and ρ_2 are frequency independent and for only one homogeneous medium or one transmission-line section, the frequency response at any frequency point can be calculated from only one simulation. This can be done as follows: the scattering coefficients, given in this simple problem by $(\rho_1\rho_2)^k$, are stored at every iteration of only one simulation, then the frequency response at any frequency point can be calculated by summing up the products of the scattering coefficient at iteration k and the propagation factor $e^{-j\beta\ell}$ raised to the power $2k$. The TFDTLM is basically inspired from the same concept discussed in the above simple example. However, the special feature of the TFDTLM approach introduced in this paper is that it makes it possible to extract all the frequency-domain information of interest over a relatively wide frequency range by performing only one simulation even if the reflection coefficients are complex frequency dependent and/or when dealing with inhomogeneous media with different propagation constants. In a TFDTLM mesh, the link-line impedances are derived in the frequency domain as in [4] and are chosen to model the frequency-dispersive material parameters. The electrical properties of each line are indicated by three subscripts: the first subscript d indicates normalized quantities per unit length and the two following subscripts indicate the line direction and polarization, respectively. L, R, C, and G represent series inductance, resistance, shunt capacitance, and conductance, respectively. In terms of these quantities, the characteristic impedance of a line along the y-direction carrying an x polarization is given by

$$Z_{yx} = \sqrt{\frac{R_{dyx} + j\omega L_{dyx}}{G_{dyx} + j\omega C_{dyx}}} \quad (3)$$

and the propagation constant along the line is given by

$$\gamma_{yx} = \sqrt{(R_{dyx} + j\omega L_{dyx})(G_{dyx} + j\omega C_{dyx})}. \quad (4)$$

The overall capacitance and conductance of all lines responsible for an E_x polarization should satisfy the medium permittivity and conductivity as follows:

$$(G_{dyx} + j\omega C_{dyx})\Delta y + (G_{dzx} + j\omega C_{dzx})\Delta z = (\sigma + j\omega\epsilon)S_x \quad (5)$$

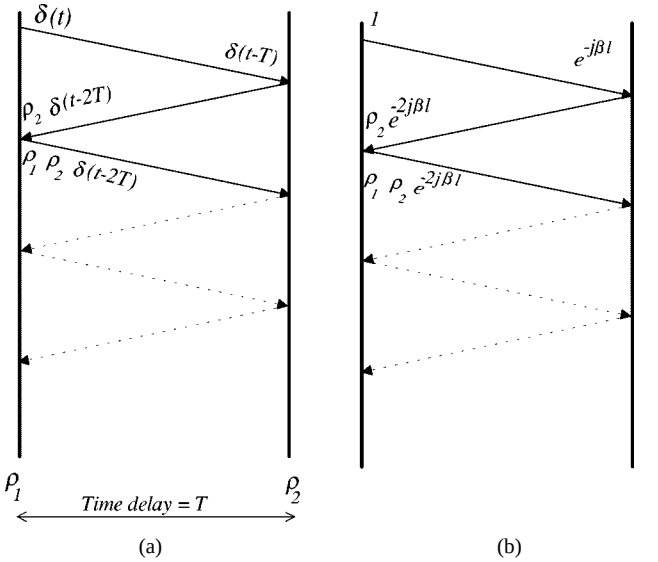

Fig. 1. (a) Bounce diagram in the time domain. (b) Equivalent frequency-domain model.

where $S_x = (\Delta y \Delta z / \Delta x)$ substitution from (3) and (4) into (5) yields

$$\frac{\gamma_{yx}\Delta y}{Z_{yx}} + \frac{\gamma_{zx}\Delta z}{Z_{zx}} = (\sigma + j\omega\epsilon)S_x. \tag{6}$$

Setting the condition

$$\begin{aligned}\gamma_{xy}\Delta x &= \gamma_{xz}\Delta x = \gamma_{yx}\Delta y = \gamma_{yz}\Delta y \\ &= \gamma_{zx}\Delta z = \gamma_{zy}\Delta z = \gamma\Delta\ell.\end{aligned} \tag{7}$$

The condition in (7) is equivalent to the synchronization condition in the TD TLM, γ is the propagation constant in the medium, and $\Delta\ell$ is an equivalent cell dimension, substituting from (7) into (6) gives

$$\frac{1}{Z_{yx}} + \frac{1}{Z_{zx}} = \frac{S_x}{Z\Delta\ell}. \tag{8}$$

Z is the intrinsic impedance of the medium given by $\sqrt{j\omega\mu/(\sigma + j\omega\epsilon)}$, and the permeability μ can be complex in case magnetic losses exist. Similar expression for the characteristic impedance of lines responsible for an E_y or an E_z polarization can be obtained using expressions similar to (5). The inductance and resistance of all the link lines responsible for an I_x current must satisfy

$$(R_{dyz} + j\omega L_{dyz})\Delta y + (R_{dzy} + j\omega L_{dzy})\Delta z = j\omega\mu S_x \tag{9}$$

substituting from (3), (4), and (7) into (9) yields

$$Z_{yz} + Z_{zy} = Z\frac{S_x}{\Delta\ell} \tag{10}$$

similarly, for the link lines responsible for I_y and I_z, expressions similar to (10) can be obtained. Equations (11a) and (11b) represent a general formulation of the set of equations that need to be satisfied in order to completely model all the constitutive parameters of the medium. The following equations include compensating open-circuit stubs added to equations similar to (8) and short-circuit stubs added to equations similar to (10):

$$\begin{aligned}\frac{1}{\hat{Z}_{yx}} + \frac{1}{\hat{Z}_{zx}} + \hat{Y}_{ox} &= \frac{S_x}{\Delta\ell} \\ \frac{1}{\hat{Z}_{xy}} + \frac{1}{\hat{Z}_{zy}} + \hat{Y}_{oy} &= \frac{S_y}{\Delta\ell} \\ \frac{1}{\hat{Z}_{xz}} + \frac{1}{\hat{Z}_{yz}} + \hat{Y}_{oz} &= \frac{S_z}{\Delta\ell}\end{aligned} \tag{11a}$$

$$\begin{aligned}\hat{Z}_{yz} + \hat{Z}_{zy} + \hat{Z}_{sx} &= \frac{S_x}{\Delta\ell} \\ \hat{Z}_{zx} + \hat{Z}_{xz} + \hat{Z}_{sy} &= \frac{S_y}{\Delta\ell} \\ \hat{Z}_{yx} + \hat{Z}_{xy} + \hat{Z}_{sz} &= \frac{S_z}{\Delta\ell}\end{aligned} \tag{11b}$$

where $\hat{Z}$ denotes an impedance normalized to the complex intrinsic impedance of the medium. The equations above are similar to the set of equations for the link-line inductances and capacitances required to satisfy the medium permeability and permittivity, respectively, in a TD TLM node. The only difference is that the link-line impedances as well as those of the compensating stubs, if any, in the TFDTLM are allowed to be complex. In addition, the equations above not only satisfy the medium permeability and permittivity, but the electric and magnetic losses as well. The above set of equations can be satisfied in more than one way. One way is to choose the link-line impedances to satisfy (11a) with no open-circuited stubs, thereby exactly modeling the medium permittivity and conductivity. Compensating short-circuited stubs with complex characteristic impedance in (11b) are then used to compensate the deficiency in satisfying the medium permeability and magnetic losses. This would be the frequency-domain equivalent of type II HSCN [6]. Another alternative is to satisfy (11b) with no short-circuited stubs for the medium permeability and magnetic losses and the deficiency in satisfying the medium permittivity and electric losses can then be compensated by open-circuited stubs of complex characteristic impedance in (11a). A third alternative is to satisfy the six equations simultaneously in a way similar to the SSCN, as in [7] and [8], with no compensating stubs. This alternative is always recommended in the TFDTLM to reduce computations. It is worth mentioning that for a uniform cell, the normalized impedance of all link lines will be identical and equal to unity. Moreover, the equivalent cell dimension $\Delta\ell$ will be equal $= 0.5\Delta x = 0.5\Delta y = 0.5\Delta z$, the factor of 1/2 confirms that the velocity of the bulk waves on the transmission-line mesh is one-half the velocity of the waves on the individual transmission lines, which agrees with the slow-wave nature of a TD TLM mesh that was also demonstrated for John's FDTLM [4]. Irrespective of the method used to solve for the link-line impedances, (11a) and (11b) show that, for one homogeneous medium, the link-line normalized impedances are all frequency independent and, consequently, so is the scattering matrix of the TFDTLM. The scattering procedure will be identical to the TD TLM. In the connection procedure, however, transition from one node to the next is accounted for through multiplication by the factor $e^{-\gamma\Delta\ell}$, which means that, from one iteration to the next, the scattered pulses are modified by the factor $e^{-\gamma\Delta\ell}$ to become incident on the next neighboring cell. In a TFDTLM node, the multiplication by the propagation factor is not actually performed at every iteration. Instead, only the scattering coefficients at the observation point are stored at every iteration. The scattering coefficients are equivalent to the impulse response of a TD TLM mesh at the same position and the corresponding iteration, except for the fact that these coefficients in the TFDTLM can be complex. The TFDTLM frequency response at the observation point at a particular frequency can then be obtained from these scattering coefficients as follows: the value stored at the first iteration is multiplied by $e^{-\gamma\Delta\ell}$. The value at the second iteration is multiplied by $e^{-2\gamma\Delta\ell}$, and so on. The final result can then be obtained by summing. It is important to note that the frequency dependence of the frequency response at the observation point is only contributed by multiplication by the factors $e^{-k\gamma\Delta\ell}$, a procedure that is only done at the end of the simulation to calculate the response at a particular frequency. This indicates that even though the TFDTLM is a frequency-domain method, performing only one simulation is enough to calculate the frequency response at any frequency of interest as long as there is only one homogeneous medium. Even in case of problems having inhomogeneous regions with different propagation

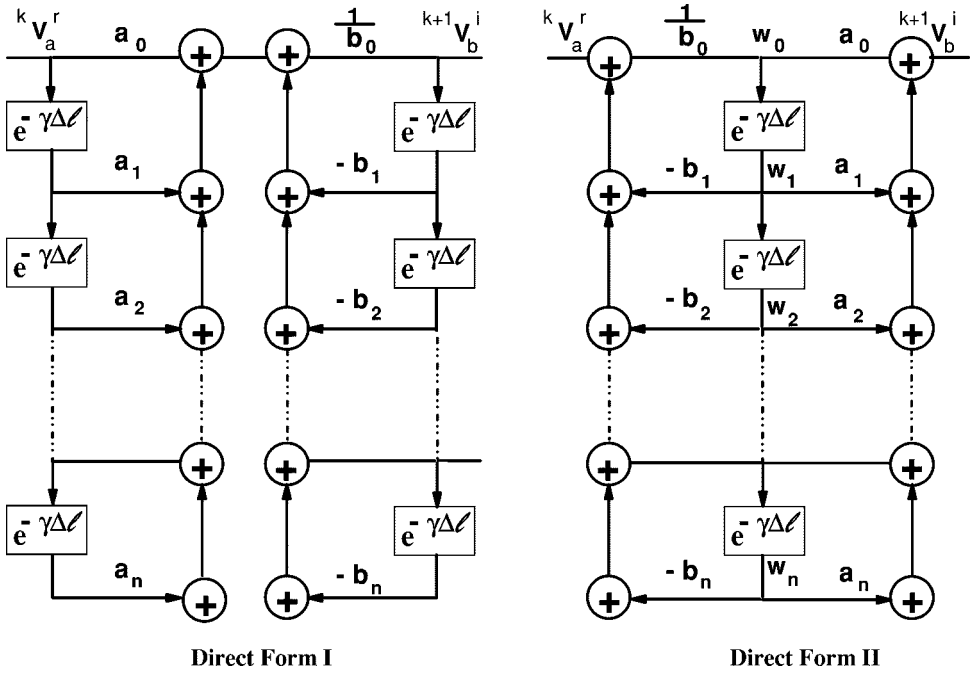

Fig. 2. Implementation of the approximation filter in a TFDTLM mesh.

constants in different regions as well as frequency-dependent reflection coefficients, the TFDTLM approach can still be applied to extract all the frequency information of interest from only one simulation. This will be discussed in Section III.

III. TFDTLM in an Inhomogeneous Medium

The technique used to overcome the problem of inhomogeneous media, multiple propagation factors, and frequency-dependent reflection coefficients involves approximating all propagation factors in each and every medium in a TFDTLM mesh in terms of the propagation factor of some reference medium chosen to be the medium with the least propagation delay. Consider having two media 1 and 2 with propagation constants γ_1 and γ_2, respectively, and effective cell dimensions $\Delta\ell_1$ and $\Delta\ell_2$, respectively, and medium 1 has the least propagation delay. The propagation constant in medium 2 is then approximated in terms of the propagation constant in medium 1 as

$$e^{-\gamma_2\Delta\ell_2} \approx e^{-m\gamma_1\Delta\ell_1}\frac{a_0+a_1e^{-\gamma_1\Delta\ell_1}\cdots+a_ne^{-n\gamma_1\Delta\ell_1}}{b_o+b_1e^{-\gamma_1\Delta\ell_1}\cdots+b_ne^{-n\gamma_1\Delta\ell_1}},\quad m=0,1,2,\cdots;\quad n=1,2,\cdots. \tag{12}$$

The filter coefficients a_n and b_n are then obtained by minimizing the mean square error between the actual propagation factor of the medium and the approximated propagation factor over the frequency range of interest. It is important to note that the filter coefficients can be complex, but are not frequency dependent. The integer m is chosen to provide extra phase change (increase filter order) that can be implemented with significantly fewer computations than by increasing the integer n. Assuming $m=1$, this technique is implemented in a TLM mesh in a way similar to the implementation of a digital filter in a digital filter processing application [9]. Fig. 2 shows two possible ways of implementing the filter. Direct form II involves less computations than direct form I and less storage as well. For this reason, direct form II was chosen to be implemented in the TFDTLM scheme. Consider a link line in medium 2 between cells a and b. In a TD TLM mesh, the connection between the two adjacent cells is implemented as follows:

$$v_b^i\big((k+1)\Delta t\big) = v_a^r(k\Delta t). \tag{13}$$

In the TFDTLM, the equivalent expression will be in the form

$${}^{k+1}V_b^i = e^{-\gamma_2\Delta\ell_2}\,{}^kV_a^r \tag{14}$$

where k is the iteration number. Assuming medium 1 is the reference medium, the propagation constant in medium 2 is approximated in terms of that of medium 1. For $m=1$, then from direct form II realization of (12), the incident voltage at node b at iteration $k+1$ can be obtained in terms of the reflected voltage at node a at iteration k as follows:

$$w_0^k = \frac{1}{b_0}\Big[{}^kV_a^r - b_1w_1^k - b_2w_2^k\cdots - b_nw_n^k\Big] \tag{15}$$

$${}^{k+1}V_b^i = e^{-\gamma_1\Delta\ell_1}\Big[a_ow_o^k + a_1w_1^k + a_2w_2^k + \cdots + a_nw_n^k\Big]. \tag{16}$$

In an actual simulation, the multiplication by the factor $e^{-\gamma_1\Delta\ell_1}$, which accounts for the transition from one iteration to the next, is not performed at every iteration. Instead, only the term inside the bracket in (16) is stored at each iteration. It is important to note that this term can be complex, but is not frequency dependent. Again, the frequency dependence of the frequency response at the observation point is only contributed by multiplication by the factors $e^{-k\gamma\Delta\ell}$. These multiplications are only done at the end of the simulation, where the frequency response at the observation point at a particular frequency is obtained by multiplying the value stored at iteration 1 by $e^{-\gamma\Delta\ell}$ and that at iteration 2 by $e^{-2\gamma\Delta\ell}$, etc. These terms are then summed to obtain the overall frequency response at the frequency point of

interest. The values of the intermediate variables w_n are first initialized to zero and then updated at each iteration by pushing them one step downwards to simulate the multiplication by the factor $e^{-\gamma\Delta\ell}$

$$w_n^{k+1} = w_{n-1}^k \quad w_{n-1}^{k+1} = w_{n-2}^k \quad \cdots \quad w_1^{k+1} = w_0^k. \quad (17)$$

By the same token, complex frequency-dependent reflection coefficients at the interface between two different media can also be approximated by a similar filter and implemented the same way.

IV. Dispersion in TFDTLM

The dispersion behavior of the TFDTLM scheme can be analyzed in the same way as in TD TLM [10]–[13], where the dispersion characteristic of a general TLM mesh can be derived by solving an eigenvalue equation given by

$$\det[I - PST] = 0. \quad (18)$$

The matrix P has a similar form to that in the TD TLM, except for the fact that propagation constants or wavenumbers along the three coordinate directions can be complex for a lossy medium. These propagation constants are written as γ_x, γ_y, and γ_z for the x-, y-, and z-directions, respectively. The matrix T is a diagonal matrix with nonzero elements equal to $e^{-\gamma\Delta\ell}$ where γ is the approximated propagation constant of the medium. To simplify the analysis, (18) is solved numerically for a two-dimensional (2-D) propagation case in the xy-plane and only for the modes associated with the three field components H_z, E_x, and E_y. The dispersion relation of conventional stub-loaded TD TLM nodes can be derived from the general condition in (18). The dispersion equation is solved numerically for both the TFDTLM and TD TLM and the error in the propagation vector is compared. The dispersion error refers to the error between the mesh propagation constant k and the actual propagation constant of the medium k_m. The dispersion error is calculated at a frequency where the cell dimension is 0.1 times the corresponding wavelength.

A. Dispersion in a Lossless Inhomogeneous Medium

The cell is assumed to be uniform having $d_x = d_y = d_z = 2\Delta\ell = 0.5$ cm. In the TFDTLM, a first-order approximation filter is used. The reference medium is considered free space with $\gamma_1 = j\omega\sqrt{\mu_0\epsilon_0}$. The filter coefficients are optimized in a frequency range where the maximum cell dimension is less than or equal to 0.125 times the corresponding wavelength. The filter is denoted by F_1 and has the form

$$F_1 = {}^{-\gamma_1\Delta\ell_1}\left(\frac{a_0 + a_1 e^{-\gamma_1\Delta\ell_1}}{b_0 + b_1 e^{-\gamma_1\Delta\ell_1}}\right). \quad (19)$$

Fig. 3 compares the percentage dispersion error calculated for a type-II HSCN and the TFDTLM in a lossless medium with $\epsilon_r = 4$. The dispersion error is plotted versus the angle from the x-axis (θ). From Fig. 3, it appears that dispersion error of the TFDTLM has a minimum of 0% and a maximum of 0.42% and an average of 0.1%, whereas that of the type-II HSCN has a minimum magnitude of 0.2% and maximum magnitude of 0.59% and an average of 0.21%. Hence, it appears that even for a lossless medium, the TFDTLM scheme still showed some improvement over type-II HSCN. It is worth mentioning that, in the results predicted in Fig. 3, the fact that the dispersion behavior for stub-loaded TLM nodes is polarization dependent, and has not been taken into consideration. For stub-loaded TLM nodes, different modes of propagation will be associated with different dispersion errors. For the case considered, we have looked into the three field components E_x, E_y, and H_z and because type-II HSCN employs short-circuited stubs that directly affect the H-fields, it is expected that, for the three field components chosen, the error associated with this node should be at a minimum. On the other hand, for the modes associated with E_z, H_y, and H_x, the error should be at a maximum. Hence, the average error should be higher than that predicted in Fig. 3. On the other hand, because the TFDTLM in the above analysis did not employ any stubs, the dispersion error is unique irrespective of the mode of propagation. This property as in the SSCN would make it easier to correct for the dispersion error [8]. Fig. 4 shows similar results to those in Fig. 3, but with $\epsilon_r = 16$. The filter approximation used with the TFDTLM has the same form in (19). This figure shows that the behavior of the HSCN continues to degrade by increasing the relative dielectric constant. The TFDTLM, on the other hand, almost maintains the same order of accuracy. It is worth noting that even for such a relatively high relative dielectric constant, a first-order approximation filter in the TFDTLM can still provide almost the same order of accuracy as with lower relative dielectric constants. This conclusion can have a significant effect on improving the computational efficiency of the TFDTLM.

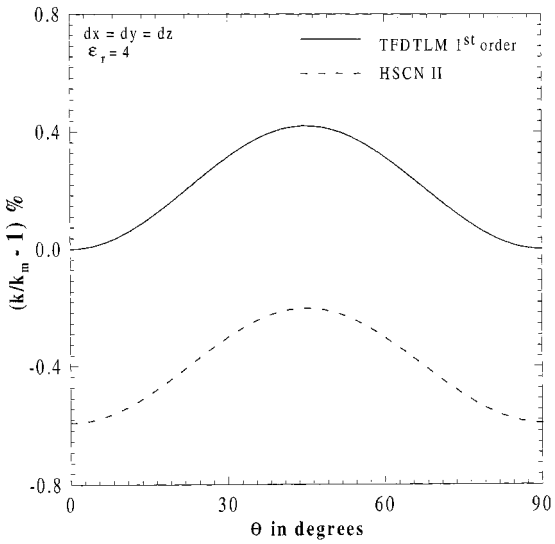

Fig. 3. Comparison between the dispersion properties of the TFDTLM and HSCN II for a uniform cell with $\epsilon_r = 4$.

B. Dispersion in Lossy Inhomogeneous Medium

In this section, the dispersion behavior of the TFDTLM in a lossy inhomogeneous medium with a uniform cell is analyzed. First- and second-order approximation filters are used. The reference medium is free space and the filter coefficients are optimized in a frequency range where the maximum cell dimension

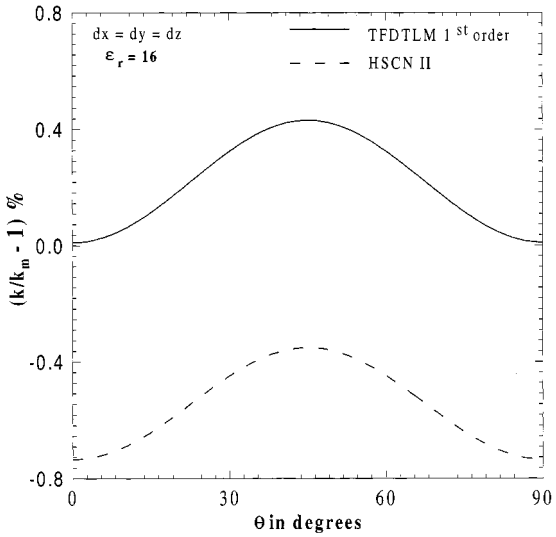

Fig. 4. Comparison between the dispersion properties of the TFDTLM and HSCN II for a uniform cell with $\epsilon_r = 16$.

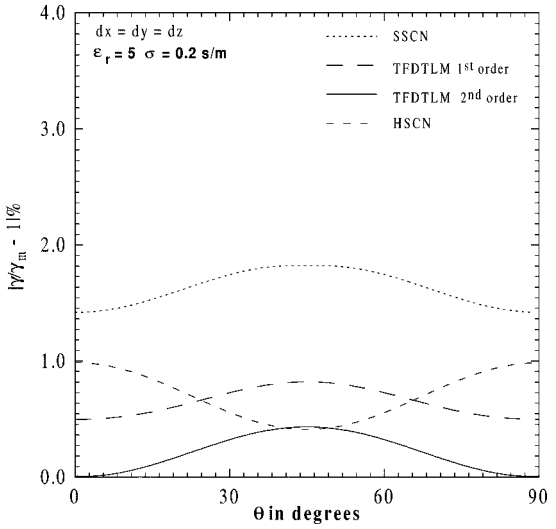

Fig. 5. Comparison between the dispersion properties of the TFDTLM, SSCN, and HSCN II in a lossy inhomogeneous medium with $\epsilon_r = 5$, $\sigma = 0.2$ S/m for a uniform cell.

is less than 0.125 times the corresponding wavelength. The filters are denoted by F_1 and F_2 for a first- and second-order approximation, respectively, and are given by

$$F_1 = e^{-\gamma_1 \Delta \ell_1} \left(\frac{a_0 + a_1 e^{-\gamma_1 \Delta \ell_1}}{b_0 + b_1 e^{-\gamma_1 \Delta \ell_1}} \right)$$

$$F_2 = e^{-\gamma_1 \Delta \ell_1} \left(\frac{a_0 + a_1 e^{-\gamma_1 \Delta \ell_1} + a_2 e^{-2\gamma_1 \Delta \ell_1}}{b_0 + b_1 e^{-\gamma_1 \Delta \ell_1} + b_2 e^{-2\gamma_1 \Delta \ell_1}} \right). \quad (20)$$

Fig. 5 shows a comparison of the dispersion characteristics of the SSCN, the HSCN II, and first- and second-order TFDTLM in a lossy medium with $\epsilon_r = 5$ and $\sigma = 0.2$ S/m (a loss tangent of about 0.3 at the considered frequency). This figure shows that the SSCN has a relatively poor dispersion characteristics for a lossy inhomogeneous medium. The first-order TFDTLM provides significant improvement over the SSCN, and a little improvement over the HSCN II. A second-order TFDTLM, on the other hand, has a superior performance over both the SSCN and HSCN II. Table I compares the minimum, maximum, and average magnitude error in the SSCN, HSCN II, and first- and second-order TFDTLM.

TABLE I
COMPARISON BETWEEN THE DISPERSION PROPERTIES OF THE TFDTLM, HSCN II, AND SSCN IN A LOSSY INHOMOGENEOUS MEDIUM WITH $\epsilon_r = 5$ AND $\sigma = 0.2$ S/m FOR A UNIFORM CELL

ε_r = 5, σ = 0.2 S/m	min | err |	max |err|	avg | err|
SSCN	1.42 %	1.82 %	1.62 %
HSCN II	0.41 %	0.98 %	0.72 %
1st order TFDTLM	0.5 %	0.82 %	0.64 %
2nd order TFDTLM	0.01 %	0.43 %	0.2 %

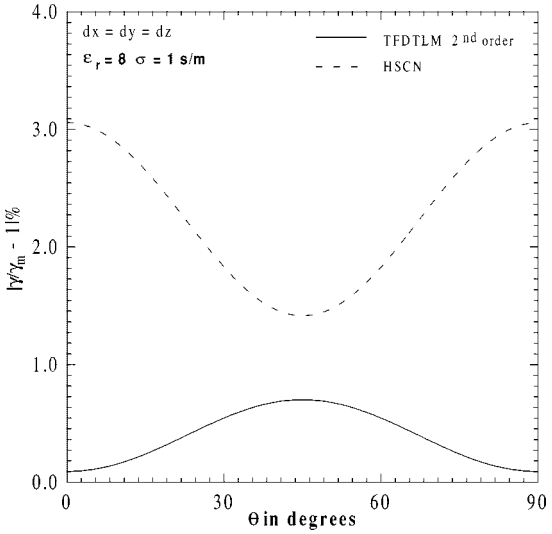

Fig. 6. Comparison between the dispersion properties of the TFDTLM and HSCN II in a lossy inhomogeneous medium with $\epsilon_r = 8$, $\sigma = 1$ S/m for a uniform cell.

Fig. 6 shows a comparison of the dispersion behavior of the HSCN II and a second-order TFDTLM for a higher loss tangent. The relative dielectric constant is chosen to be eight with a conductivity σ of 1 S/m, a loss tangent of about one, at the operating frequency. This figure shows that the behavior of the HSCN is significantly degraded. The TFDTLM, on the other hand, almost maintains the same order of accuracy as in a lossless homogeneous medium with a very slight degradation. Another important conclusion can also be derived from the results in Fig. 6. It has been shown that a second-order approximation filter can provide an acceptable order of accuracy for a lossy inhomogeneous medium with relatively high losses. This conclusion was verified for different combinations of medium parameters with relatively high loss tangents.

C. Dispersion in a Lossy Inhomogeneous Medium with a Nonuniform Cell

In this section, a lossy inhomogeneous medium with a nonuniform cell will be considered. The TFDTLM can handle the situation of a nonuniform cell in a simple and direct way. Equations (11a) and (11b) are functions of the normalized

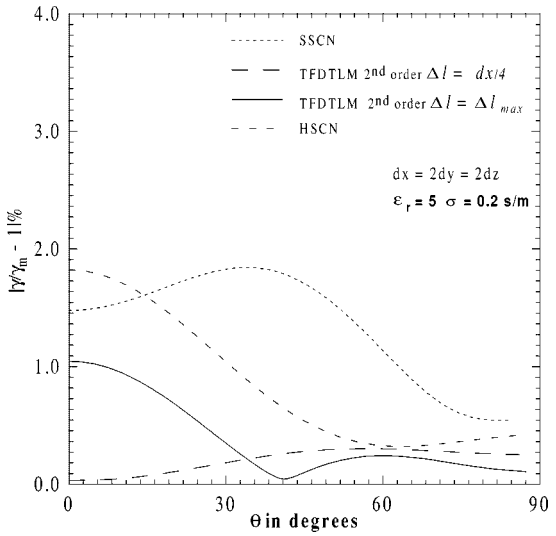

Fig. 7. Comparison between the dispersion properties of the TFDTLM, SSCN, and HSCN II in a lossy inhomogeneous medium with $\epsilon_r = 5$, $\sigma = 0.2$ S/m for a nonuniform cell.

link-line impedances (normalized by the complex intrinsic impedance of the medium) and the equivalent cell dimension $\Delta\ell$. In order to account for nonuniform cells, the set of equations are solved simultaneously with no stubs as in the SSCN for the normalized link-line impedances and the equivalent cell dimension $\Delta\ell$. The reason they are chosen to be solved the same way as in the SSCN is that the SSCN proved to have superior dispersion characteristics in a homogenous lossless medium with nonuniform cells [8]. The set of equations can, in general, be solved as in a general symmetrical condensed node (GSCN), as illustrated in [14], for optimum dispersion behavior in a nonuniform cell. The solution of (11a) and (11b) implicitly assumes that the propagation delay along any cell dimension is equal to the propagation delay in the medium. The role of the TFDTLM becomes significant in approximating the propagation constant in different media with different frequency-dependent material parameters in terms of the propagation constant of some reference medium. Fig. 7 compares the dispersion behavior of a second-order TFDTLM, SSCN, and the HSCN in a lossy inhomogeneous medium having $\epsilon_r = 5$ and $\sigma = 0.2$ S/m. The cell is assumed to be nonuniform having $d_x = 2d_y = 2d_z = 1$ cm. It is important to mention that there is no limitation to the use of a graded mesh in the TFDTLM. In the TFDTLM, the set of link-line impedances are chosen to account for the nonuniform cell dimension by solving the set of equations in (11a) and (11b) with no stubs. A second-order approximation filter is then used to approximate the medium propagation factor in terms of that of the reference medium. The reference medium is taken to be free space. The filter coefficients are optimized in a frequency range where the maximum cell dimension is less than 0.125 times the corresponding wavelength. In the SSCN, the link-line impedances are chosen to account for the nonuniform cell and satisfy the medium dielectric constant. Lossy stubs are added to account for losses. The SSCN, as shown in Fig. 7, has the worst dispersion behavior, followed by the HSCN. The TFDTLM shows significant improvement over the HSCN even when both are operating at the maximum permissible equivalent cell dimension, the maximum equivalent cell dimension that would guarantee all normalized link-line impedances are positive. The maximum permissible equivalent cell dimension in the HSCN is simply the maximum permissible time step multiplied by the speed of light in air. It is worth mentioning that the maximum permissible equivalent cell dimension in the TFDTLM is equal to almost 1.2 times that required by the HSCN, i.e., the number of iterations required by the TFDTLM is less than 85% of that required by the HSCN. When the equivalent cell dimension is dropped to 0.25 d_x, which is the same as that required by the HSCN, Fig. 7 shows that the dispersion of the TFDTLM is significantly improved.

TABLE II
COMPARISON OF THE PERCENTAGE ERROR IN THE Q-FACTOR ESTIMATION OBTAINED FROM THE HSCN AND TFDTLM FOR $\epsilon_r = 5$, $\sigma = 0.05$ S/m

	HSCN			TFDTLM		
$f_{o\ actual}$ (GHz)	f_o	Q	% err	f_o	Q	% err
1.9	1.88	10.7	2.4	1.9	10.4	-0.98
3	2.99	17.6	6.1	2.99	16.6	-0.1
4.24	4.24	26.7	13	4.2	24.2	3.4
4.84	4.75	31.5	21	4.78	27.9	-5.3
5.53	5.6	38	22	5.52	29.3	-3

V. SIMULATION RESULTS

A lossy cavity of size 5 cm × 5 cm × 5 cm was simulated with a uniform grid using the TFDTLM. The cavity is filled with a dielectric with $\epsilon_r = 5$ and conductivity equals 0.05 S/m. The quality factors are calculated for the HSCN and the TFDTLM approach and compared with the theoretical values. A second-order approximation filter was used for the TFDTLM. The filter coefficients were optimized up to a frequency where the maximum cell dimension is in the order of 0.18 times the wavelength in a medium with $\epsilon_r = 5$. This range is guaranteed to cover the frequency range over which the TLM is always operated for a given cell dimension. Table II shows a comparison between the accuracy of the type-II HSCN and TFDTLM. The results in Table II prove that the TFDTLM provides improved accuracy in calculating the quality factor and, consequently, in modeling the losses in the medium. Both the TFDTLM and HSCN have an acceptable order of accuracy in the low-frequency range, although the TFDTLM is still better. As the frequency increases, the HSCN significantly degrades, whereas the TFDTLM almost maintains the same order of accuracy with very slight degradation.

VI. ON THE COMPUTATIONAL EFFICIENCY OF THE TFDTLM

It has been mentioned earlier that as compared to a FDTLM scheme, where the intensity of computation per frequency is approximately of the same order, the TFDTLM would be computationally more efficient. The reason is that, in the TFDTLM, all

TABLE III
COMPARISON OF THE NUMBER OF MULTIPLICATION AND ADDITIONS IN A TD TLM AND FIRST- AND SECOND-ORDER TFDTLM

		TFDTLM	
	TD TLM	1st order	2nd order
# of real multip.	18	126	222
# real add./sub.	54	180	276

the frequency-domain information in the entire frequency range of interest can be extracted from only one simulation. In a traditional FDTLM, on the other hand, the simulation has to repeated at every frequency point. As compared to a TD TLM scheme, the TFDTLM is less efficient. The reason is that, in a TFDTLM, all the computations must be complex. Also, more complex computations are used for the implementation of the approximation filter. In what follows, the number of multiplications and additions in the TFDTLM will be compared to that required in a TD TLM. The storage requirement will be compared as well. The following calculations for a TD TLM will be based on a general node having six different link-line impedances for different coordinate directions and polarizations, six stubs, and six lossy stubs. For the TFDTLM, six different link-line impedances are considered with neither lossy, inductive, nor capacitive stubs. For the TFDTLM, all the filter coefficients are normalized to b_0 in (12), i.e., b_0 is taken to be unity. It is important to note that, in the following calculations, every full complex multiplication, i.e., multiplication of two complex numbers, is converted to four equivalent real multiplications and two equivalent real additions. On the other hand, multiplication of a real and a complex number is equivalent to two real multiplications. The complex class developed in C++ could actually differentiate between these two types of multiplications and, hence, improve the computational efficiency of a TFDTLM code. Table III summarizes the total number of real multiplications and additions for a first- and second-order TFDTLM as compared to a TD TLM. The numbers for the TD TLM are based on the efficient computation algorithm for the GSCN given in [15].

It is important to note that, in the region that is treated as a reference medium in a TFDTLM, the connection procedure does not involve any approximation filter. This would drop the equivalent number of real multiplication in this region to 30 and the number of equivalent real additions to 84. Consequently, the overall number of multiplications and additions will be reduced. Concerning the memory storage requirement of a TFDTLM, a first-order TFDTLM will require 24 complex memory locations per node, as opposed to 18 real memory locations in a TD TLM with six stubs. A second-order TFDTLM, on the other hand, will require 36 complex memory locations per node.

VII. SUMMARY AND CONCLUSIONS

In this paper, a novel FDTLM approach was introduced. The new approach is based on a steady-state analysis in the frequency domain using transient analysis techniques. The TFDTLM has the advantage of being able to extract all the frequency-domain information in the frequency range of interest from only one simulation. This special feature of the TFDTLM makes it computationally more efficient as compared to any other FDTLM. The TFDTLM was found to have less dispersion error than the TD TLM in modeling lossless as well as lossy inhomogeneous media with uniform and nonuniform cells. For the TFDTLM, it has been shown that a first-order approximation filter can perfectly model lossless inhomogeneous media, whereas a second-order approximation filter can provide an acceptable order of accuracy even for a lossy inhomogeneous medium with a relatively high loss tangent. The TFDTLM was tested in a simple lossy cavity simulation and was able to better estimate the quality factors than traditional TD TLM. The computational intensity and the storage requirement of the TFDTLM were also estimated. It is important to note that one interesting property of the TFDTLM is that it can easily be interfaced with any TD TLM method. Therefore, in lossless regions with relatively low relative dielectric constants and/or permeabilities, a traditional TD TLM technique can be used. The TFDTLM can then be used only for regions with frequency-dependent material properties, relatively high permittivities, permeabilities, and/or high loss tangents. This would consequently save a lot of computations and help improve the overall computational efficiency of the TFDTLM.

REFERENCES

[1] I. Salama and S. Riad, "A new computationally efficient frequency domain TLM," in *2nd Int. TLM Theory Applicat. Workshop*, Munich, Germany, Oct. 1997.
[2] H. Jins and R. Vahldieck, "The frequency domain transmission line matrix—A new concept," *IEEE Trans. Microwave Theory Tech*, vol. 40, pp. 2207–2218, Dec. 1992.
[3] D. P. Johns, A. J. Wlodarcyzk, A. Mallik, and C. Christopoulos, "New TLM Technique for steady state field solutions in three dimensions," *Electron. Lett.*, vol. 28, no. 18, pp. 1692–1694, 1992.
[4] D. P. Johns and C. Christopoulos, "A new frequency domain TLM method for the numerical solution of steady state electromagnetic problems," *Proc. Inst. Elect. Eng.*, vol. 141, no. 4, pp. 310–316, July 1994.
[5] V. Trenkic, C. Christopoulos, and T. M. Benson, "Simple and elegant formulation of scattering in TLM nodes," *Electron. Lett.*, pp. 1651–1652, Sept. 1993.
[6] P. Berini and K. Wu, "A pair of hybrid symmetrical condensed node," *IEEE Microwave Guided Wave Lett.*, vol. 4, pp. 244–246, July 1994.
[7] V. Trenkic, C. Christopoulos, and T. M. Benson, "New symmetrical super condensed node for TLM method," *Electron. Lett.*, vol. 30, no. 4, pp. 329–330, Feb. 1994.
[8] ——, "Generally graded mesh using the symmetrical super condensed node," *Electron. Lett.*, vol. 30, no. 10, pp. 795–797, May 1994.
[9] A. Oppenheim and R. W. Schafer, *Discrete-Time Signal Processing*. Englewood Cliffs, NJ: Prentice-Hall, 1989.
[10] J. S. Nielsen and W. J. R. Hoefer, "Generalized dispersion analysis and spurious modes of 2-D and 3-D TLM formulations," *IEEE Trans. Microwave Theory Tech.*, vol. 11, pp. 2207–2218, Aug. 1993.
[11] ——, "A complete dispersion analysis of the condensed node TLM mesh," *IEEE Trans. Magn.*, vol. 27, pp. 3982–3985, Sept. 1991.
[12] J. A. Morente, G. Gimenez, J. A. Porti, and M. Khalladi, "Dispersion analysis for a TLM mesh of symmetrical condensed nodes with stubs," *IEEE Trans. Microwave Theory Tech.*, vol. 43, pp. 452–456, Feb. 1995.
[13] M. Celuch-Marcysiak and W. K. Gwarek, "On the effect of bilateral dispersion in inhomogeneous symmetrical condensed node modeling," *IEEE Trans. Microwave Theory Tech.*, vol. 42, pp. 1069–1073, June 1994.
[14] V. Trenkic, C. Christopoulos, and T. M. Benson, "Development of a general symmetrical condensed node for the TLM method," *IEEE Trans. Microwave Theory Tech.*, vol. 44, pp. 2129–2135, Dec. 1996.
[15] ——, "Efficient computation algorithms for TLM," in *1st Int. TLM Theory Applicat. Workshop*, Victoria, B.C., Canada, Aug. 1995, pp. 77–80.

Iman Salama was born in Cairo, Egypt. She received the B.Sc. degree in electronics and telecommunications engineering (with a distinction with honor grade) and the M.Sc. degree in communications from Cairo University, Cairo, Egypt, in 1991 and 1993, respectively, and the Ph.D. degree from the Virginia Polytechnic Institute and State University, Blacksburg, in 1997.

In 1991, she joined the Electrical Engineering Department, Cairo University, Cairo, Egypt, where was involved in the area of fading compensation and capacity improvement of CDMA cellular systems. In Fall 1994, she joined the Virginia Polytechnic Institute and State University, where she was involved in the area of microwave measurements and electromagnetic simulations. Her current research interests include electromagnetics, numerical methods, microwave measurements, and signal processing.

Sedki M. Riad (M'78–SM'82–F'92) was born in Egypt, on February 19, 1946. He received the B.Sc. and M.Sc. degrees from Cairo University, Cairo, Egypt, in 1966 and 1972, respectively, both in electrical engineering, and the Ph.D. degree in engineering science from the University of Toledo, Toledo, OH, in 1976.

From 1975 to 1977, he was with the National Institute for Standards and Technology (NIST), Boulder, CO, as a Guest Worker, where he was involved with post-doctoral research. In 1985, he rejoined NIST for a six-month period, while on leave from the Virginia Polytechnic Institute and State University, Blacksburg. He has held faculty positions at Cairo University (1966–73), the University of Central Florida, Orlando (1977–79), and the King Saud University, Riyadh, Saudi Arabia (1984–85). Since 1979, he has been a Professor of electrical engineering and the Director of the Time Domain and RF Measurement Laboratory at the Virginia Polytechnic Institute and State University. He has authored and co-authored one book chapter and over 100 technical journal and conferences papers. His main area of interest is microwave measurements with emphasis in time-domain techniques, instrumentation, and related device modeling, computer simulation, and signal processing.

Dr. Riad is a Registered Professional Engineer in the State of Florida. He is a past chairman of the U.S. National Commission A of the International Union of Radio Science (URSI) (1994–1996). He has also been active with the IEEE Virginia Mountain Section and is past chairman of the section and has chaired several of its committees. He is an Editorial Review Board member of several IEEE societies, most particularly, the IEEE TRANSACTIONS ON INSTRUMENTATION AND MEASUREMENTS. He has served as the guest editor for an IMTC'92 Special Issue and he has participated in several of the I&M's two main conferences CPEM and IMTC.